MOF Composites

Deutsche Ausgabe: DOI: 10.1002/ange.201510655
Internationale Ausgabe: DOI: 10.1002/anie.201510655

Pd Nanocubes@ZIF-8: Integration of Plasmon-Driven Photothermal Conversion with a Metal–Organic Framework for Efficient and Selective Catalysis

*Qihao Yang, Qiang Xu, Shu-Hong Yu, and Hai-Long Jiang**

Abstract: *Composite nanomaterials usually possess synergetic properties resulting from the respective components and can be used for a wide range of applications. In this work, a Pd nanocubes@ZIF-8 composite material has been rationally fabricated by encapsulation of the Pd nanocubes in ZIF-8, a common metal–organic framework (MOF). This composite was used for the efficient and selective catalytic hydrogenation of olefins at room temperature under 1 atm H_2 and light irradiation, and benefits from plasmonic photothermal effects of the Pd nanocube cores while the ZIF-8 shell plays multiple roles; it accelerates the reaction by H_2 enrichment, acts as a "molecular sieve" for olefins with specific sizes, and stabilizes the Pd cores. Remarkably, the catalytic efficiency of a reaction under 60 mW cm^{-2} full-spectrum or 100 mW cm^{-2} visible-light irradiation at room temperature turned out to be comparable to that of a process driven by heating at 50 °C. Furthermore, the catalyst remained stable and could be easily recycled. To the best of our knowledge, this work represents the first combination of the photothermal effects of metal nanocrystals with the favorable properties of MOFs for efficient and selective catalysis.*

The hydrogenation of compounds with unsaturated bonds is a very common transformation involved in many chemical processes.[1] Traditionally, hydrogenation reactions are carried out with hydride reagents, for example, sodium borohydride, lithium aluminum hydride, or ammonia borane.[2] Although these reductants are effective, they are of high cost, and their decomposition leads to byproducts that are difficult to separate from the reaction system. Catalytic reduction with molecular hydrogen (H_2) obviously represents an attractive, more atom-economic alternative. Hydrogenation in the presence of H_2 typically requires high temperatures and/or H_2 pressures.[3] However, from the viewpoints of energy, environment, cost, and safety, the development of catalytic hydrogenation reactions that do not depend on the use of heat and high-pressure hydrogen gas is highly desirable.

To this end, solar energy can be utilized instead of heat to drive a reaction by making use of the surface plasmonic properties of metal nanocrystals.[4] To efficiently convert sunlight into the heat required for the hydrogenation reaction, the metal nanocrystals (e.g., Pd, one of the most active species owing to its strong interaction with H_2 molecules[3,5]) should possess sufficient plasmonic absorption cross-sections to harvest light over a broad spectral range. Pd nanocrystals with a variety of shapes have been reported, with Pd nanocubes (NCs) being one of the most active and widely studied systems.[6] It is expected that Pd NCs not only display high activity in such hydrogenation reactions but also enable the utilization of solar energy to drive the reaction by making use of their well-known surface plasmon effects.

On the other hand, the small Pd NCs are usually not uniformly dispersed and readily aggregate to some extent during the reaction, especially upon heating, which greatly impedes their catalytic performance. To address this issue, the encapsulation of Pd NCs inside porous materials as shells with small pore openings should be a judicious solution, which would offer the following advantages: 1) The Pd NCs will maintain their high dispersion inside the host materials during catalytic recycling; 2) the pore structure of the shell is beneficial to the transportation of substrates/products and guarantees the accessibility of the Pd active sites; 3) the porous shell leads to enhanced catalytic efficiency by H_2 enrichment;[7] and 4) the use of shells with different pore sizes would enable the size-selective hydrogenation of different substrates. To sieve various molecules with different sizes, the shell should display a well-defined porous structure and uniform pore sizes. In this context, metal–organic frameworks (MOFs, also called porous coordination polymers), which not only possess diversified and tailorable structures with uniform pores but can also be used for various functional applications,[8,9] especially for gas sorption, could be ideal candidates.

Bearing these facts in mind, we rationally grew a representative MOF, Zn(2-methylimidazole)$_2$ (ZIF-8),[10] on Pd NCs to obtain Pd NCs@ZIF-8 with a core–shell structure. This composite structure displays a plasmonic band covering the UV-to-visible spectral range and thus induces high temperatures to drive the hydrogenation reaction by photothermal conversion. Compared to Pd NCs with similar sizes, the catalytic activity of Pd NCs@ZIF-8 in the hydrogenation of 1-hexene under 100 mW cm^{-2} full-spectrum light irradiation at room temperature is significantly enhanced, and the reaction efficiency is even higher than that of a reaction

[*] Q. Yang, Prof. Dr. S.-H. Yu, Prof. Dr. H.-L. Jiang
Hefei National Laboratory for Physical Sciences at the Microscale
CAS Key Laboratory of Soft Matter Chemistry
Collaborative Innovation Center of Suzhou Nano Science and Technology, Department of Chemistry
University of Science and Technology of China
Hefei, Anhui 230026 (P.R. China)
E-mail: jianglab@ustc.edu.cn
Homepage: http://staff.ustc.edu.cn/~jianglab/
Prof. Dr. Q. Xu
National Institute of Advanced Industrial Science and Technology
Ikeda, Osaka 563–8577 (Japan)

Supporting information and ORCID(s) from the author(s) for this article are available on the WWW under http://dx.doi.org/10.1002/anie.201510655.

thermally heated at 50 °C. Furthermore, owing to the MOF shell, the nanocomposite catalyst shows excellent recyclability and selectivity because large olefins cannot reach the Pd active sites (Scheme 1). Although metal nanoparticles@MOF composites have been intensively studied as catalysts in recent years,[11] to the best of our knowledge, this is the first time that the plasmonic photothermal effects of metal nanocrystals were combined with the favorable properties of MOFs towards efficient and selective catalysis.

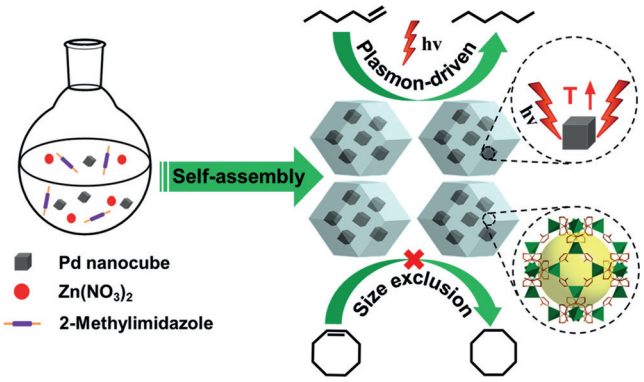

Scheme 1. Self-assembly of Pd NCs@ZIF-8 and plasmon-driven selective catalysis of the hydrogenation of olefins.

The Pd NCs were synthesized from K_2PdCl_4 as a precursor; L-ascorbic acid was used as the reductant, poly(vinyl pyrrolidone) (PVP) as a stabilizer, and KBr as a capping agent to promote the formation of {100} facets.[12] Zeolite-type ZIF-8 was chosen owing to its high stability, large surface area (BET = 1670 $m^2 g^{-1}$), high H_2 uptake capacity, and facile growth under ambient conditions. The core–shell Pd NCs@ZIF-8 composite was synthesized by introducing the as-synthesized Pd NCs into a methanol solution containing the ZIF-8 precursors ($Zn(NO_3)_2 \cdot 6H_2O$ and 2-methylimidazolate) and subsequent aging at 4 °C for one hour.

The powder X-ray diffraction (XRD) pattern of Pd NCs@ZIF-8 shows that the crystallinity and structure of ZIF-8 was well maintained upon addition of the Pd NCs (Figure 1a). The identifiable diffraction peaks for Pd NCs imply their inclusion. N_2 sorption experiments indicate that Pd NCs@ZIF-8 is highly porous, and its BET surface area was determined to be 1474 $m^2 g^{-1}$. The slight decrease in surface area compared to parent ZIF-8 is ascribed to the mass occupation by the Pd NCs (Figure 1b). H_2 sorption studies for Pd NCs@ZIF-8 at 77 K and 298 K clearly manifest its H_2 enrichment capability (Figure 1c; see also the Supporting Information, Figure S1), which should greatly improve the catalytic hydrogenation. As-synthesized Pd NCs exhibit a broad absorption band in the surface plasmon resonance (SPR) spectrum at 220–700 nm, which was also observed for the Pd NCs@ZIF-8 composite (Figure 1d).

Transmission electron microscopy (TEM) and high-resolution TEM (HRTEM) studies suggest that the Pd NCs have a well-defined structure with sizes of 17 ± 3 nm and are enclosed by {100} facets (Figures 2a,b and S2). A scanning electron microscopy (SEM) image shows the size of an individual Pd NCs@ZIF-8 particle to be 250–350 nm (Figure 2c). TEM images confirm the core–shell nanostructure of the composite material, with the Pd NCs well encapsulated by the ZIF-8 shell and retention of the shape and size of the Pd NCs (Figures 2d and S3). The thickness of the ZIF-8 shell can be controlled simply by changing the reaction time (Figure S4). An approximately 130 nm thick ZIF-8 shell, which was obtained by growth for 60 minutes, was used hereafter, unless otherwise stated. The actual Pd content of the composite was determined to be 8.7 wt % by inductively coupled plasma atomic emission spectroscopy (ICP-AES).

Encouraged by the broad SPR absorption band of the Pd NCs@ZIF-8 composite, full-spectrum light irradiation was employed to investigate its surface-plasmon-driven photothermal conversion for the catalytic hydrogenation of olefins at room temperature. 1-Hexene was used as a model substrate to optimize the reaction parameters. The catalytic performance of the Pd NCs@ZIF-8 composite in the hydrogenation

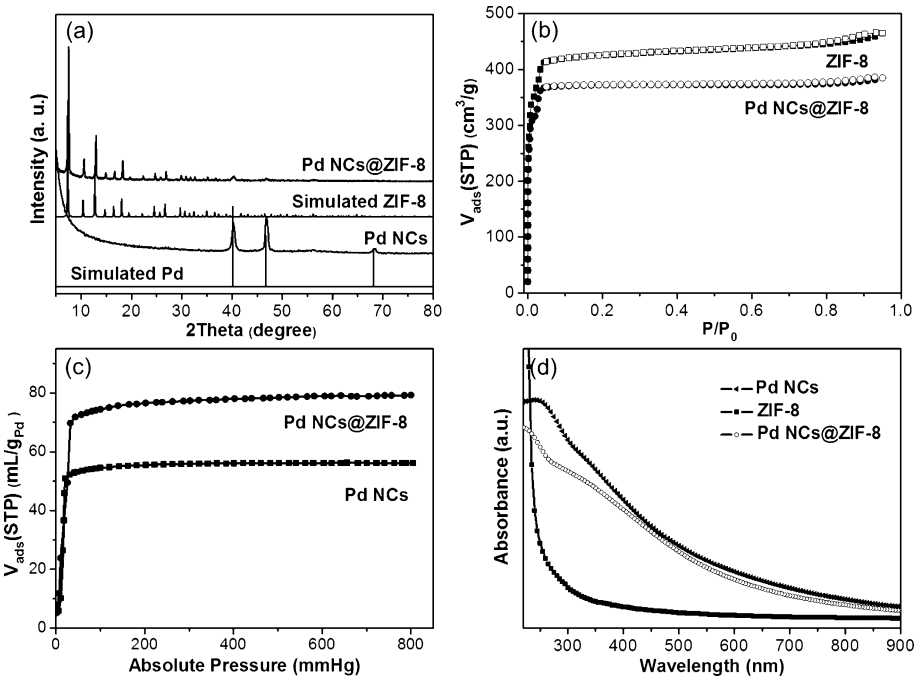

Figure 1. a) Powder XRD patterns simulated for Pd and ZIF-8 and experimentally determined for as-synthesized Pd NCs and Pd NCs@ZIF-8. b) N_2 sorption isotherms for ZIF-8 and Pd NCs@ZIF-8 at 77 K. c) H_2 sorption isotherms for Pd NCs@ZIF-8 and Pd NCs at 298 K. d) UV/Vis absorption spectra for ZIF-8, Pd NCs, and Pd NCs@ZIF-8.

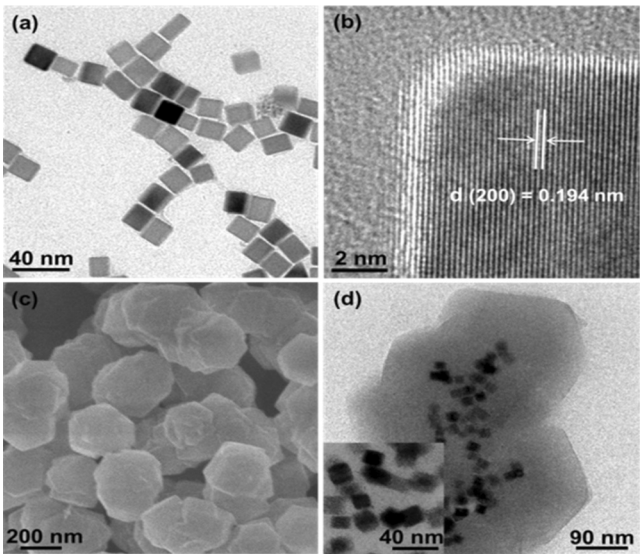

Figure 2. a) TEM and b) HRTEM images of Pd NCs. c) SEM and d) TEM images of Pd NCs@ZIF-8. Inset in (d): Pd nanocubes inside ZIF-8.

of 1-hexene under irradiation with different light intensities is illustrated in Figure 3a. In the presence of the composite, the hydrogenation product was formed in only 37% after 30 min at room temperature in the dark. Strikingly, the performance of the composite catalyst was significantly improved by full-spectrum irradiation with a 100 mW cm^{-2} Xe lamp, and the desired product was formed in 66% yield. The dispersion of accessible Pd sites was estimated to be 1.6%,[7b] based on a CO titration experiment. The turnover frequency (TOF) was calculated to be as high as 675 $mol_{1\text{-hexene}}$ mol_{Pd}^{-1} min^{-1}. The reaction yield over the composite was almost linearly dependent on the light intensity, which provides direct evidence that the improved catalytic activity is due to the light irradiation. Furthermore, the conversion of light into heat in the reaction involving Pd NCs@ZIF-8 was clearly demonstrated (Figure S5). To assess the importance of photothermal effects for the overall reaction, the catalytic hydrogenation over Pd NCs@ZIF-8 was conducted with all parameters unaltered except for changing light irradiation to heating. The results clearly show that the reaction efficiency is much better under 100 mW cm^{-2} full-spectrum irradiation than upon heating at 50°C; the conversion achieved by heating at this temperature is similar to that achieved by 60 mW cm^{-2} full-spectrum irradiation in the presence of the Pd NCs@ZIF-8 catalyst (Figures 3a and S6). As visible light accounts for approximately 50% of natural sunlight, the visible-light photothermal conversion properties of materials are very important. Under visible-light irradiation (100 mW cm^{-2}) at room temperature, the Pd NCs@ZIF-8 catalyst afforded the desired product in 52% yield, which corresponds to that achieved by heating at 50°C (Figure 3a). By deducting the yield obtained in the dark (37%), we can calculate that the visible-light irradiation contributes roughly 52% to the full-spectrum performance, which is in good agreement with the percentage of visible light in sunlight.

To examine the influence of the size of the Pd NCs on the reaction, a Pd NCs@ZIF-8 composite with small Pd NCs (7 ± 3 nm) was synthesized for comparison (Figure S7). Although small Pd nanostructures usually display higher activity, their narrower SPR absorption impacts on their plasmon-driven catalytic efficiency. The catalyst with smaller Pd NCs is indeed inferior to the original one (Pd size: 17 ± 3 nm; Figure S8). Furthermore, the thickness of the ZIF-8 shell can be controlled by changing the time of the MOF growth; a thin ZIF-8 shell was slightly beneficial to the catalytic activity (Figure S9). To exclude transport limitations, additional experiments with different amounts of the Pd NCs@ZIF-8 catalyst were conducted to determine the dependence of the yield on the catalyst amount (Figure S10). The results indicate

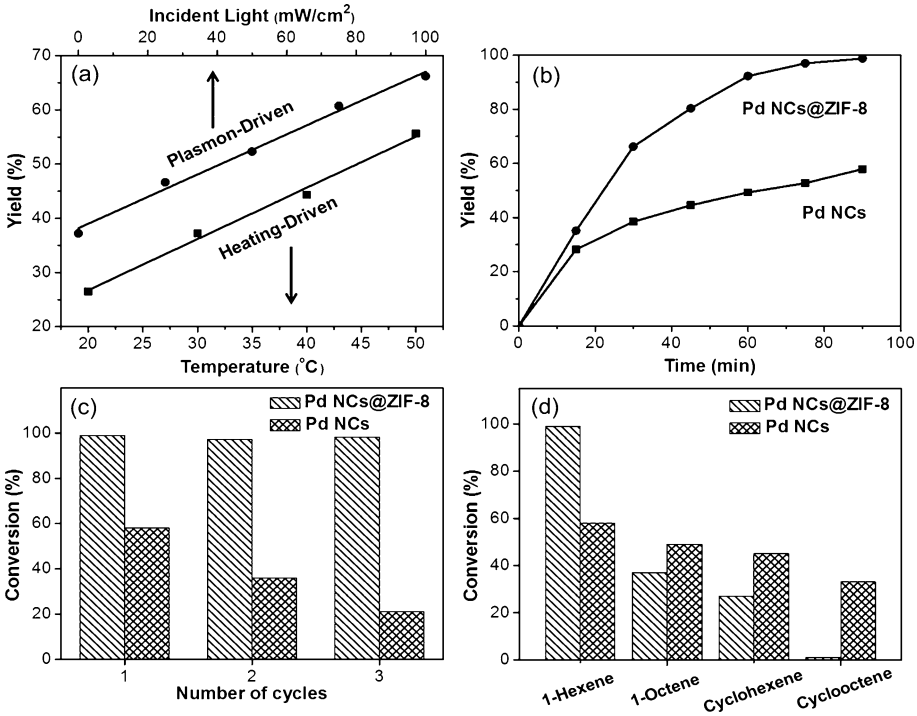

Figure 3. a) The yields of the hydrogenation of 1-hexene with 1 atm H_2 over Pd NCs@ZIF-8 under full-spectrum irradiation with different light intensities at room temperature or upon heating at different temperatures. b) Dependence of the hydrogenation yield of 1-hexene on the reaction time over Pd NCs or Pd NCs@ZIF-8. c) Recyclability of Pd NCs@ZIF-8 and Pd NCs for the hydrogenation of 1-hexene. d) Conversions of the hydrogenation of various alkenes over Pd NCs@ZIF-8 and Pd NCs. Reaction conditions in (b)–(d): 100 mW cm^{-2} full-spectrum irradiation, room temperature.

that the influence of internal mass diffusion transport resistance is negligible.

To demonstrate the advantages of the Pd NCs@ZIF-8 composite in catalysis, the control reactions over ZIF-8 or Pd NCs were also carried out. The results show that the activity of ZIF-8 is negligible (Table S1). Kinetic analysis manifests the much higher activity of Pd NCs@ZIF-8 compared to Pd NCs (Figure 3b). Under light irradiation, the use of Pd NCs@ZIF-8 leads to almost complete conversion of 1-hexene in 90 min, whereas only 58% conversion occurred in the presence of Pd NCs under otherwise identical reaction conditions. The significant difference could be partially due to the H_2 enrichment capability of ZIF-8 (as indicated above), which serves as a nanoreactor for catalysis and also as a hydrogen gas reservoir to accelerate the hydrogenation process.[7] Meanwhile, the Pd NCs are well incorporated and fixed into the ZIF-8 host, and their migration/aggregation is thus prevented. Recycling experiments clearly show that the yields over Pd NCs@ZIF-8 are close to 100% over three consecutive runs, whereas with the Pd NCs without ZIF-8 protection, the yield gradually decreased to only 21% in the third run (Figure 3c). These results are in line with the TEM observations: The Pd NCs undergo severe aggregation to large particles whereas the ZIF-8-protected Pd NCs maintain their original size/morphology and dispersion inside the MOF (Figures S11 and S12). The powder XRD profile further supports the assumption that the crystallinity of Pd NCs@ZIF-8 was well preserved (Figure S13). The Pd NCs could be hardly recovered by centrifugation owing to their small size whereas the large size of the Pd NCs@ZIF-8 composite greatly facilitates its recyclability and the heterogenization of the active sites.

Furthermore, the well-defined pore structure of the ZIF-8 shell can act as a "molecular sieve" for selective catalysis. As shown in Figure 3d, the use of Pd NCs@ZIF-8 leads to significantly different conversions for olefins with different molecular sizes. For 1-hexene, approximately 100% conversion can be achieved in 90 minutes, which is even better than that achieved with Pd NCs (58% yield only), inferring that the ZIF-8 shell does not affect the diffusion of 1-hexene (molecular size ca. 2.5 Å). The slightly larger 1-octene (ca. 4 Å) and cyclohexene (ca. 4.2 Å) hardly pass through the ZIF-8 shell with a pore aperture of 3.4 Å, and therefore, the yields decreased to 37% and 27%, respectively, after 90 min. When the substrate size becomes even larger, such as with cyclooctene (ca. 5.5 Å), negligible activity was observed. In stark contrast, the conversions are similar for all four substrates over the Pd NCs, reflecting the size selectivity of the Pd NCs@ZIF-8 catalyst. This observation further confirms that all Pd NCs are encapsulated inside ZIF-8, which is consistent with our TEM results. ICP-AES analysis confirmed that negligible leaching (< 0.02% Pd leaching from the catalyst) had occurred after hydrogenation.

In summary, we have rationally fabricated a core–shell Pd NCs@ZIF-8 composite that benefits from surface-plasmon-driven photothermal effects of the Pd NCs and the specific properties of the MOF, which accelerates the catalytic reaction by H_2 enrichment, enables the selection of substrates of a specific size for selective catalysis, and stabilizes the Pd NCs for excellent recyclability. As a result, the composite selectively catalyzes the hydrogenation of small olefins under light irradiation at room temperature. Compared to thermally driven catalytic hydrogenation at 50 °C, 100 mW cm^{-2} visible-light irradiation afforded similar catalytic activity whereas 100 mW cm^{-2} full-spectrum irradiation led to a much higher efficiency in the absence of additional heating. The superior catalytic performance can be ascribed to the broad absorption band of the Pd NCs and many accessible active Pd sites on corner and edge positions. Impressively, thanks to the stabilization endowed by the ZIF-8 shell, the nanostructure and crystallinity of the catalyst, but also its catalytic activity, were well maintained during recycling experiments. This work represents the first attempt on utilizing solar energy for accelerating a catalytic reaction by combining the SPR effects of metal nanocrystals with the favorable properties of MOFs, which would exert their synergistic advantages and open up an avenue to the utilization of solar energy instead of heat to drive a heterogeneous catalytic reaction.

Acknowledgements

This work was supported by the NSFC (21371162, 51301159, and 21521001), the 973 program (2014CB931803), the NSF of Anhui Province (1408085MB23), the Recruitment Program of Global Youth Experts, and the Fundamental Research Funds for the Central Universities (WK2060190026).

Keywords: heterogeneous catalysis · metal–organic frameworks · microporous materials · palladium nanocubes · photothermal effects

How to cite: *Angew. Chem. Int. Ed.* **2016**, *55*, 3685–3689
Angew. Chem. **2016**, *128*, 3749–3753

[1] a) X. Cui, K. Burgess, *Chem. Rev.* **2005**, *105*, 3272–3296; b) A. M. Smith, R. Whyman, *Chem. Rev.* **2014**, *114*, 5477–5510.
[2] a) P. Hervés, M. Pérez-Lorenzo, L. M. Liz-Marzán, J. Dzubiella, Y. Lu, M. Ballauff, *Chem. Soc. Rev.* **2012**, *41*, 5577–5587; b) Q. Yang, Y.-Z. Chen, Z. U. Wang, Q. Xu, H.-L. Jiang, *Chem. Commun.* **2015**, *51*, 10419–10422; c) X. Yang, L. Zhao, T. Fox, Z.-X. Wang, H. Berke, *Angew. Chem. Int. Ed.* **2010**, *49*, 2058–2062; *Angew. Chem.* **2010**, *122*, 2102–2106; d) T. N. Gieshoff, M. Villa, A. Welther, M. Plois, U. Chakraborty, R. Wolf, A. Jacobi von Wangelin, *Green Chem.* **2015**, *17*, 1408–1413; e) H. Göksu, S. F. Ho, O. Metin, K. Korkmaz, A. M. Garcia, M. S. Gültekin, S. H. Sun, *ACS Catal.* **2014**, *4*, 1777–1782.
[3] a) Y. Wang, J. Yao, H. Li, D. Su, M. Antonietti, *J. Am. Chem. Soc.* **2011**, *133*, 2362–2365; b) J. Chen, R. Liu, Y. Guo, L. Chen, H. Gao, *ACS Catal.* **2015**, *5*, 722–733; c) C. Zhao, J. He, A. A. Lemonidou, X. Li, J. A. Lercher, *J. Catal.* **2011**, *280*, 8–16; d) H. Liu, T. Jiang, B. Han, S. Liang, Y. Zhou, *Science* **2009**, *326*, 1250–1252.
[4] a) Y. Sun, *Adv. Funct. Mater.* **2010**, *20*, 3646–3657; b) Q. Zhang, D. Q. Lima, I. Lee, F. Zaera, M. Chi, Y. Yin, *Angew. Chem. Int. Ed.* **2011**, *50*, 7088–7092; *Angew. Chem.* **2011**, *123*, 7226–7230; c) S. Linic, U. Aslam, C. Boerigter, M. Morabito, *Nat. Mater.* **2015**, *14*, 567–576; d) F. Wang, C. Li, H. Chen, R. Jiang, L.-D. Sun, Q. Li, J. Wang, J. C. Yu, C.-H. Yan, *J. Am. Chem. Soc.* **2013**, *135*, 5588–5601; e) S. Sarina, E. R. Waclawik, H. Zhu, *Green Chem.* **2013**, *15*, 1814–1833; f) L. M. Liz-Marzán, C. J. Murphy,

J. Wang, *Chem. Soc. Rev.* **2014**, *43*, 3820 – 3822; g) Z. Li, J. J. Foley, S. Peng, C.-J. Sun, Y. Ren, G. P. Wiederrecht, S. K. Gray, Y. Sun, *Angew. Chem. Int. Ed.* **2015**, *54*, 8948 – 8951; *Angew. Chem.* **2015**, *127*, 9076 – 9079.

[5] a) S. Kidambi, J. Dai, J. Li, M. L. Bruening, *J. Am. Chem. Soc.* **2004**, *126*, 2658 – 2659; b) O. M. Wilson, M. R. Knecht, J. C. Garcia-Martinez, R. M. Crooks, *J. Am. Chem. Soc.* **2006**, *128*, 4510 – 4511.

[6] a) R. Long, K. Mao, X. Ye, W. Yan, Y. Huang, J. Wang, Y. Fu, X. Wang, X. Wu, Y. Xie, Y. Xiong, *J. Am. Chem. Soc.* **2013**, *135*, 3200 – 3207; b) M. Jin, H. Zhang, Z. Xie, Y. Xia, *Energy Environ. Sci.* **2012**, *5*, 6352 – 6357; c) S.-B. Wang, W. Zhu, J. Ke, M. Lin, Y.-W. Zhang, *ACS Catal.* **2014**, *4*, 2298 – 2306.

[7] a) Z. Zhang, Y. Chen, X. Xu, J. Zhang, G. Xiang, W. He, X. Wang, *Angew. Chem. Int. Ed.* **2014**, *53*, 429 – 433; *Angew. Chem.* **2014**, *126*, 439 – 443; b) Z. Li, R. Yu, J. Huang, Y. Shi, D. Zhang, X. Zhong, D. Wang, Y. Wu, Y. Li, *Nat. Commun.* **2015**, *6*, 8248.

[8] a) G. Férey, C. Mellot-Draznieks, C. Serre, F. Millange, *Acc. Chem. Res.* **2005**, *38*, 217 – 225; b) J. R. Long, O. M. Yaghi, *Chem. Soc. Rev.* **2009**, *38*, 1213 – 1214; c) H.-C. Zhou, J. R. Long, O. M. Yaghi, *Chem. Rev.* **2012**, *112*, 673 – 674; d) H.-C. Zhou, S. Kitagawa, *Chem. Soc. Rev.* **2014**, *43*, 5415 – 5418.

[9] a) Y. He, W. Zhou, G. Qian, B. Chen, *Chem. Soc. Rev.* **2014**, *43*, 5657 – 5678; b) S. Ma, H.-C. Zhou, *Chem. Commun.* **2010**, *46*, 44 – 53; c) J. Gascon, A. Corma, F. Kapteijn, F. X. Llabrés i Xamena, *ACS Catal.* **2014**, *4*, 361 – 378; d) T. Zhang, W. Lin, *Chem. Soc. Rev.* **2014**, *43*, 5982 – 5993; e) J. Lee, O. K. Farha, J. Roberts, K. A. Scheidt, S. T. Nguyen, J. T. Hupp, *Chem. Soc. Rev.* **2009**, *38*, 1450 – 1459; f) Z. Q. Wang, S. M. Cohen, *Chem. Soc. Rev.* **2009**, *38*, 1315 – 1329; g) D. Farrusseng, S. Aguado, C. Pinel, *Angew. Chem. Int. Ed.* **2009**, *48*, 7502 – 7513; *Angew. Chem.* **2009**, *121*, 7638 – 7649; h) K. Khaletskaya, J. Reboul, M. Meilikhov, M. Nakahama, S. Diring, M. Tsujimoto, S. Isoda, F. Kim, K. I. Kamei, R. A. Fischer, S. Kitagawa, S. Furukawa, *J. Am. Chem. Soc.* **2013**, *135*, 10998 – 11005; i) B. Van de Voorde, B. Bueken, J. Denayer, D. De Vos, *Chem. Soc. Rev.* **2014**, *43*, 5766 – 5788; j) Y. Fu, D. Sun, Y. Chen, R. Huang, Z. Ding, X. Fu, Z. Li, *Angew. Chem. Int. Ed.* **2012**, *51*, 3364 – 3367; *Angew. Chem.* **2012**, *124*, 3420 – 3423; k) Y. Zhao, N. Kornienko, Z. Liu, C. Zhu, S. Asahina, T.-R. Kuo, W. Bao, C. Xie, A. Hexemer, O. Terasaki, P. Yang, O. M. Yaghi, *J. Am. Chem. Soc.* **2015**, *137*, 2199 – 2202; l) D. Wisser, F. M. Wisser, S. Raschke, N. Klein, M. Leistner, J. Grothe, E. Brunner, S. Kaskel, *Angew. Chem. Int. Ed.* **2015**, *54*, 12588 – 12591; *Angew. Chem.* **2015**, *127*, 12776 – 12780; m) X. Liu, L. He, J. Zheng, J. Guo, F. Bi, X. Ma, K. Zhao, Y. Liu, R. Song, Z. Tang, *Adv. Mater.* **2015**, *27*, 3273 – 3277.

[10] a) K. S. Park, Z. Ni, A. P. Côté, J. Y. Choi, R. Huang, F. J. Uribe-Romo, H. K. Chae, M. O'Keeffe, O. M. Yaghi, *Proc. Natl. Acad. Sci. USA* **2006**, *103*, 10186 – 10191; b) X.-C. Huang, Y.-Y. Lin, J.-P. Zhang, X.-M. Chen, *Angew. Chem. Int. Ed.* **2006**, *45*, 1557 – 1559; *Angew. Chem.* **2006**, *118*, 1587 – 1589.

[11] a) S. Hermes, M.-K. Schröter, R. Schmid, L. Khodeir, M. Muhler, A. Tissler, R. W. Fischer, R. A. Fischer, *Angew. Chem. Int. Ed.* **2005**, *44*, 6237 – 6241; *Angew. Chem.* **2005**, *117*, 6394 – 6397; b) Y. K. Hwang, D. Hong, J.-S. Chang, S. H. Jhung, Y.-K. Seo, J. Kim, A. Vimont, M. Daturi, C. Serre, G. Férey, *Angew. Chem. Int. Ed.* **2008**, *47*, 4144 – 4148; *Angew. Chem.* **2008**, *120*, 4212 – 4216; c) H.-L. Jiang, B. Liu, T. Akita, M. Haruta, H. Sakurai, Q. Xu, *J. Am. Chem. Soc.* **2009**, *131*, 11302 – 11303; d) B. Yuan, Y. Pan, Y. Li, B. Yin, H. Jiang, *Angew. Chem. Int. Ed.* **2010**, *49*, 4054 – 4058; *Angew. Chem.* **2010**, *122*, 4148 – 4152; e) G. Lu, S. Li, Z. Guo, O. K. Farha, B. G. Hauser, X. Qi, Y. Wang, X. Wang, S. Han, X. Liu, J. S. DuChene, H. Zhang, Q. Zhang, X. Chen, J. Ma, S. C. J. Loo, W. D. Wei, Y. Yang, J. T. Hupp, F. Huo, *Nat. Chem.* **2012**, *4*, 310 – 316; f) Y. Huang, S. Liu, Z. Lin, W. Li, X. Li, R. Cao, *J. Catal.* **2012**, *292*, 111 – 117; g) J. Hermannsdörfer, M. Friedrich, N. Miyajima, R. Q. Albuquerque, S. Kümmel, R. Kempe, *Angew. Chem. Int. Ed.* **2012**, *51*, 11473 – 11477; *Angew. Chem.* **2012**, *124*, 11640 – 11644; h) H. R. Moon, D. W. Lim, M. P. Suh, *Chem. Soc. Rev.* **2013**, *42*, 1807 – 1824; i) A. Dhakshinamoorthy, H. Garcia, *Chem. Soc. Rev.* **2012**, *41*, 5262 – 5284; j) X.-H. Liu, J.-G. Ma, Z. Niu, G.-M. Yang, P. Cheng, *Angew. Chem. Int. Ed.* **2015**, *54*, 988 – 991; *Angew. Chem.* **2015**, *127*, 1002 – 1005; k) Y.-Z. Chen, Y.-X. Zhou, H. Wang, J. Lu, T. Uchida, Q. Xu, S.-H. Yu, H.-L. Jiang, *ACS Catal.* **2015**, *5*, 2062 – 2069; l) P. Hu, J. Zhuang, L.-Y. Chou, H. K. Lee, X. Ling, Y.-C. Chuang, C.-K. Tsung, *J. Am. Chem. Soc.* **2014**, *136*, 10561 – 10564; m) Y. Liu, Z. Tang, *Adv. Mater.* **2013**, *25*, 5819 – 5825.

[12] M. Jin, H. Liu, H. Zhang, Z. Xie, J. Liu, Y. Xia, *Nano Res.* **2011**, *4*, 83 – 91.

Received: November 17, 2015
Revised: January 2, 2016
Published online: January 21, 2016

